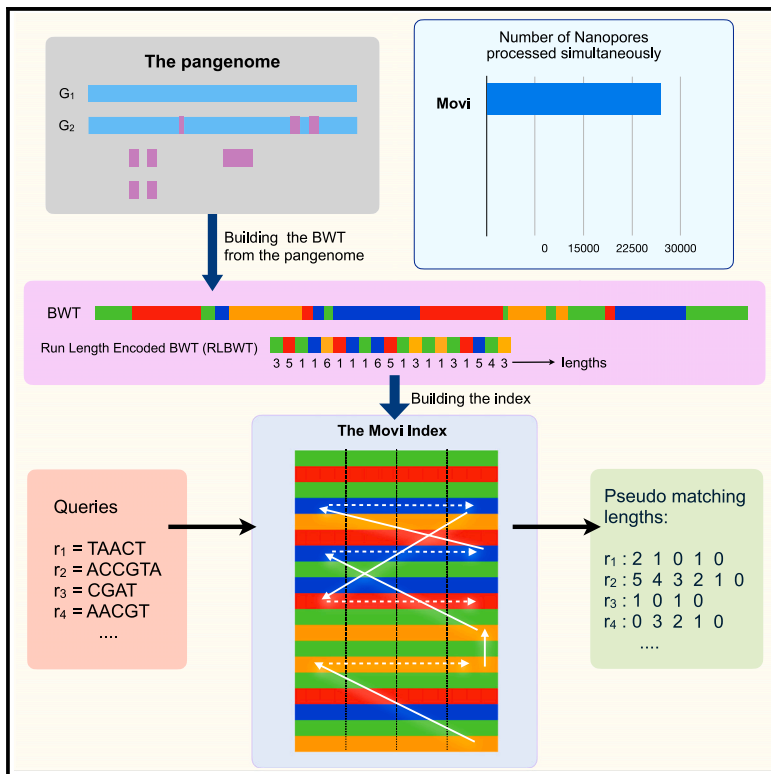


# Movi: A fast and cache-efficient full-text pangenome index

## Graphical abstract



## Authors

Mohsen Zakeri, Nathaniel K. Brown,  
Omar Y. Ahmed, Travis Gagie,  
Ben Langmead

## Correspondence

mzakeri1@jhu.edu (M.Z.),  
langmea@cs.jhu.edu (B.L.)

## In brief

Biocomputational method; Classification of bioinformatical subject; Genomic analysis

## Highlights

- Movi is a very fast and cache-efficient index for pangenomes
- The size of Movi's index scales with the non-redundant content in the pangenome
- A single Movi thread can handle output from 26,890 nanopores
- Movi builds on the move structure, a full-text compressed index that uses the BWT



## Article

# Movi: A fast and cache-efficient full-text pangenome index

Mohsen Zakeri,<sup>1,\*</sup> Nathaniel K. Brown,<sup>1</sup> Omar Y. Ahmed,<sup>1</sup> Travis Gagie,<sup>2</sup> and Ben Langmead<sup>1,3,\*</sup>

<sup>1</sup>Department of Computer Science, Johns Hopkins University, Baltimore, MD 21218, US

<sup>2</sup>Faculty of Computer Science, Dalhousie University, Halifax, NS B3H 4R2, Canada

<sup>3</sup>Lead contact

\*Correspondence: mzakeri1@jhu.edu (M.Z.), langmea@cs.jhu.edu (B.L.)

<https://doi.org/10.1016/j.isci.2024.111464>

## SUMMARY

Pangenome indexes are promising tools for many applications, including classification of nanopore sequencing reads. Move structure is a compressed-index data structure based on the Burrows-Wheeler Transform (BWT). It offers simultaneous  $O(1)$ -time queries and  $O(r)$  space, where  $r$  is the number of BWT runs (consecutive sequence of identical characters). We developed Movi based on the move structure for indexing and querying pangenomes. Movi scales very well for repetitive text as its size grows strictly by  $r$ . Movi computes sophisticated matching queries for classification such as pseudo-matching lengths and backward search up to 30 times faster than existing methods by minimizing the number of cache misses and using memory prefetching to attain a degree of latency hiding. Movi's fast constant-time query loop makes it well suited to real-time applications like adaptive sampling for nanopore sequencing, where decisions must be made in a small and predictable time interval.

## INTRODUCTION

Pangenome indexes are promising tools for aligning and classifying sequencing reads with respect to large sets of similar reference sequences. While many existing tools are k-mer based,<sup>1,2</sup> others use flexible indexes enabling arbitrary-length pattern matching queries, like the FM-index<sup>3,4</sup> and r-index.<sup>5,6</sup> The FM-index<sup>7</sup> and r-index<sup>8</sup> are full-text indexes that facilitate matching via “backward search.” The r-index can also find maximal exact matches (MEMs) and matching statistics using the MONI algorithm.<sup>9</sup> Unlike the FM-index, the r-index is run-length compressed, allowing the index to grow proportionally to the amount of *distinct* sequence (Table 1) in a pangenome reference, rather than its total length.

In practice, the r-index comprises a collection of data structures such as bitvectors and wavelet tries. A single query such as a backward-search step involves memory accesses to many disparate memory addresses within these structures. The number and unpredictability of these accesses leads to cache misses, i.e., pauses during which the processor is stalled waiting for portions of the data structures to be moved from main memory to nearby cache memories. Even when the time required for an index query is theoretically constant, the latency incurred by cache misses can be large, making queries slow in practice. Variability in the number of cache misses incurred per query leads to fluctuating latency across queries. Overall, the effect is to make queries slow with high variability.

The Move structure was introduced by Nishimoto and Tabei in 2021.<sup>10</sup> Like the FM-index and r-index, it is a full-text index

based on the Burrows-Wheeler Transform (BWT). It achieves both  $O(r)$  space usage and  $O(1)$  (constant) time for matching queries, where  $r$  is the number of runs in the BWT of the text. This combination has not been achieved by other indexes; e.g., the r-index can achieve one or the other but not both. Another key advantage of the move structure is that it consists entirely of a single table as shown in **STAR Methods** (Figure 1). Move structure queries need only perform a limited number of accesses to this table, incurring few—usually just one or two—cache misses per query. That is, move structure queries have excellent locality of reference. This leads to faster queries with more predictable latency compared to alternatives like the r-index. Although past studies have shown some of the move structure's computational trade-offs relative to r-index,<sup>11</sup> no studies have investigated these advantages related to speed and locality of reference.

Here, we introduce Movi, a pangenome full-text index based on the move structure. Movi is much faster than alternative pangenome indexes like the r-index. We measure Movi's cache characteristics and show that queries achieve a small, nearly minimal number of cache misses. Further, we show that the latency of the remaining cache misses can be “hidden” to a large degree by rearranging the computation and using memory prefetch instructions, as explained in **STAR Methods** (Figure 2). We demonstrate that Movi can implement the same algorithms as alternative pangenome tools like r-index (backward search) and SPUMONI (pseudo-matching lengths and matching statistics), while running drastically faster, e.g., 30 times faster than SPUMONI. Finally, we show that despite having a larger size compared to other pangenome indexes, Movi's index grows



**Table 1. Total number of distinct k-mers and the number of BWT runs for an increasing number of bacteria genomes**

# of bacteria genomes	Length (n)	# of k-mers	# of BWT runs (r)	n/r
7	58,161,474	28,574,428	40,406,317	1.44
(~ $\frac{1}{5}$ of the genomes) 1,530	14,178,369,894	200,298,516	231,715,345	61.19
(~ $\frac{2}{5}$ of the genomes) 3,060	28,453,355,796	277,080,392	319,250,083	89.13
(~ $\frac{3}{5}$ of the genomes) 4,590	42,690,972,294	320,277,549	368,768,962	115.77
(~ $\frac{4}{5}$ of the genomes) 6,120	56,878,399,936	360,992,370	415,457,305	136.91
(All the genomes) 7,692	71,502,400,380	393,168,219	452,717,159	157.94

The first row contains one genome from each of the seven bacterial species, with each subsequent row including approximately one-fifth more of the data. The BWT is built over the forward and reverse complement of genomes. Both the forward and reverse complement of each k-mer are represented by a single canonical k-mer (the lexicographically smaller k-mer).

more slowly than other pangenome indexes as genomes are added.

In short, Movi is the fastest available tool for full-text pangenome indexing and querying, and our open source implementation enables its application in various classification and alignment scenarios, including in speed-critical scenarios like adaptive sampling for nanopore sequencing.

## RESULTS

We measured Movi's speed and cache characteristics relative to the related SPUMONI approach as well as to other approaches that use the FM index (Bowtie 2), a pangenome k-mer index (Fulgor), or other approaches that achieve compression (minimap2). We measure the predictability of Movi's innermost loop, to

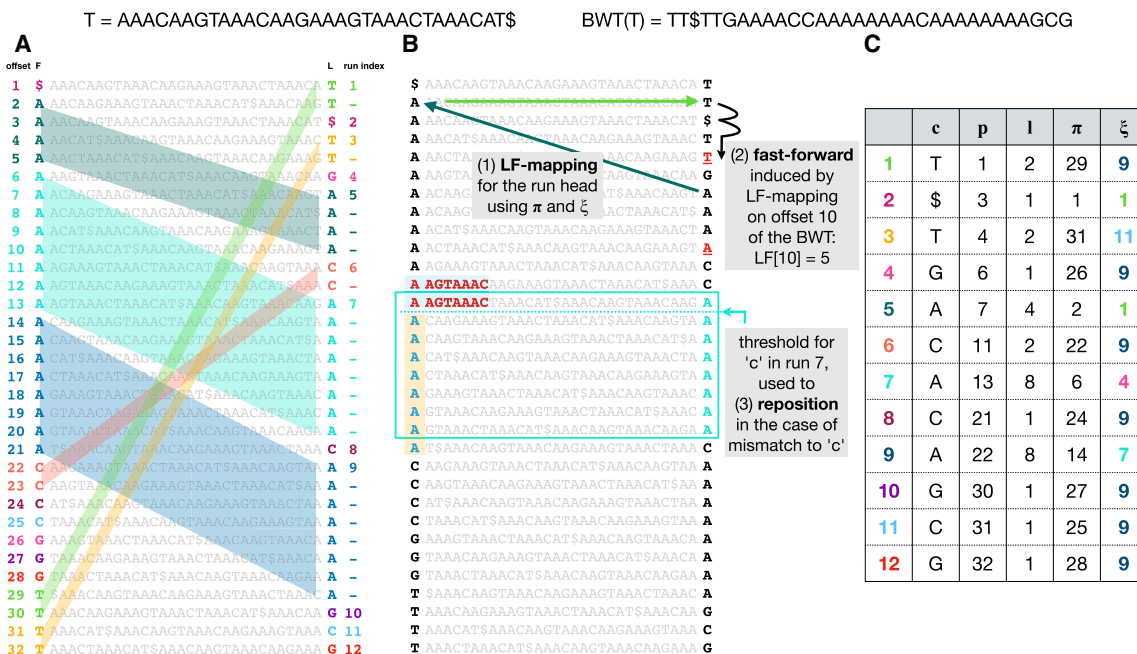


**Figure 1. Top: T and BWT(T)**

(A) BWT(T), consisting of T's sorted rotations. The leftmost column is called F, and the rightmost column is BWT(T), also called L. Distinct BWT runs are given distinct colors. The LF-mapping maps these runs to same-letter stretches in F. This is illustrated using matching colors and, in the case of multi-character runs, by parallelograms connecting BWT characters to their counterparts in F.

(B) Arrows at the top illustrate how a move-structure query for LF[10] results in one LF step (green arrows) followed by two fast forward steps (black arrow). Below, the blue arrows illustrate how a threshold facilitates “repositioning.” A mismatch between the BWT character (“A”) and a “C” from the query causes a jump to the nearest offset above or below ending in “C.” The one above was chosen in this case because it has a longer longest common prefix (LCP) with the rotation at the original offset. The threshold (blue dotted line) denotes the point above which rows have a longer LCP with the next C-terminated row above, but rows below have a longer LCP with the next C-terminated row below (with ties broken arbitrarily).

(C) Each BWT run is a row in the move structure table; c is the run character,  $\ell$  is the length, p is the offset with respect to the BWT,  $\pi$  is LF[p], and  $\xi$  is the index of the run containing offset  $\pi$ .

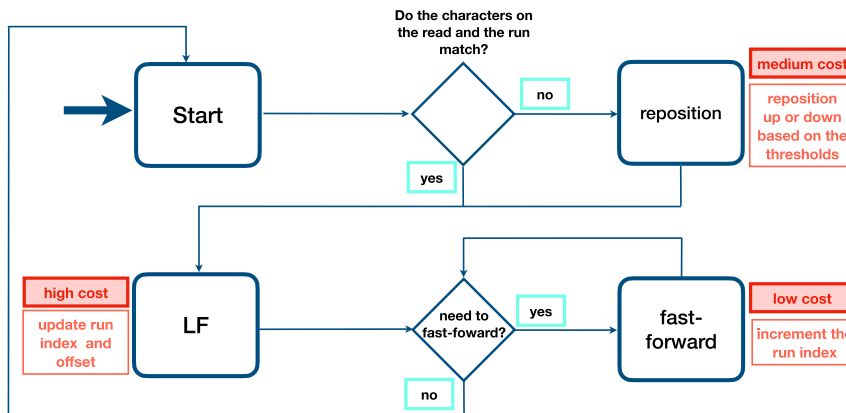


**Figure 2. Schematic of PML computation with Movi**

The typical cost associated with each memory access is shown. Higher costs are incurred by accesses that move long distances to memory addresses that have not been used recently.

assess its utility for real-time data processing applications. Finally, we explore how Movi's index scales when applied to genomes from the Human Pan-genome Reference Consortium (HPRC).<sup>12</sup> Experiments were run on 3 GHz Intel Xeon Gold Cascade Lake 6248R CPU with 1.5TB DDR4 memory.

#### Pseudo-matching lengths for a mock community

We first measured the move structure's efficiency for computing pseudo-matching lengths (PMLs), an approximation of matching statistics previously shown to be useful for classification tasks, including adaptive sampling.<sup>5,6</sup> We compared Movi's default and constant modes to SPUMONI in terms of index size and query time. We also included SPUMONI2 in our comparison, which applies a minimizer digestion on the sequences. This approach reduces the lengths of both queries and reference sequence, which results in faster queries and a smaller index size, even though the accuracy of the classification drops marginally.<sup>6</sup> We ran the tools on the Zymo High Molecular Weight Mock Microbial Community (NCBI: SRR11071395) previously used to evaluate Uncalled.<sup>13</sup>

For further context, we also evaluated the FM-index-based tool Bowtie2, the minimizer and Hashtable-based tool minimap2, and the colored compacted De Bruijn-graph-based tool

Fulgor. Note that these tools differ in what they actually compute, with Bowtie2 and minimap2 generating full read alignments and Fulgor producing pseudo-alignments. The sample consists of about 800K long reads sequenced by Oxford Nanopore Technologies (ONT) with the average length of 15K bases.

For all tools, the index consisted of all the complete reference genomes of seven bacteria species (*Bacillus subtilis*, *Enterococcus faecalis*, *Escherichia coli*, *Listeria monocytogenes*, *Pseudomonas aeruginosa*, *Salmonella enterica*, and *Staphylococcus aureus*). These were all obtained from RefSeq database.<sup>14</sup>

Table 2 shows the size of the indexes built by all the tools as well as the time required for querying all the reads. We first compared the computational requirements of Movi-default to SPUMONI. We observed that Movi-default was 30 times faster than SPUMONI, but its index was 4.7 times larger than SPUMONI's. We observe that the minimizer digestion improves the speed and index size of SPUMONI2 compared to SPUMONI; however, Movi-default is still 12 times faster than SPUMONI2. The minimizer digestion could be utilized in Movi (or in other tools) to achieve a similar speed and index-size improvement as well. Since we want to focus on evaluating the performance of different index types, rather than the specific modifications on the alphabet, we will only consider the SPUMONI version without the minimizer digestion for the rest of the experiments in this manuscript. Movi-constant was both slower and had a larger index compared to Movi-default; as we show later, however, the Movi-constant mode benefits from more predictable performance across inner-loop iterations.

**Table 2. Indexes are built over all available complete genomes of seven bacteria from the RefSeq database, with a total of 7,692 genomes**

Tool	Index type	Full-text	Query type	Color	Size (GB)	Query time (hh:mm:ss)
Movi-default	Move structure	Yes	PML	No	8.5	00:18:40
Movi-constant	Move structure	Yes	PML	No	14	00:24:01
SPUMONI	r-index	Yes	PML	No	1.8	09:20:55
SPUMONI2	r-index + digestion	Yes	PML	No	0.82	03:45:08
Bowtie2	FM-index	Yes	Alignments	Yes	12x2 + 40 <sup>b</sup>	–
Minimap2	Minimizers	No	Alignments	Yes	68	21:31:28 <sup>a</sup>
Fulgor	ccdbg (kmers)	No	Pseudo-alignments	Yes	0.65 + 2.34 <sup>c</sup>	01:11:51

The size of the FASTA file, including the reverse complement, is 67 GB, containing 71,502,400,380 base pairs. There are 452,717,159 runs in the BWT of the reference sequence. The number of long reads in the sample is 800K.

<sup>a</sup>The minimap2 is run with 16 threads unlike other tools that are run with a single thread.

<sup>b</sup>12x2 shows the size of two FM-indexes in the Bowtie2's index (the forward and reverse strand).

<sup>c</sup>The size of the Fulgor's index is broken down into two parts; the size of the k-mer set is 0.65 GB, and the size of the index related to the document (color) information is 2.34 GB.

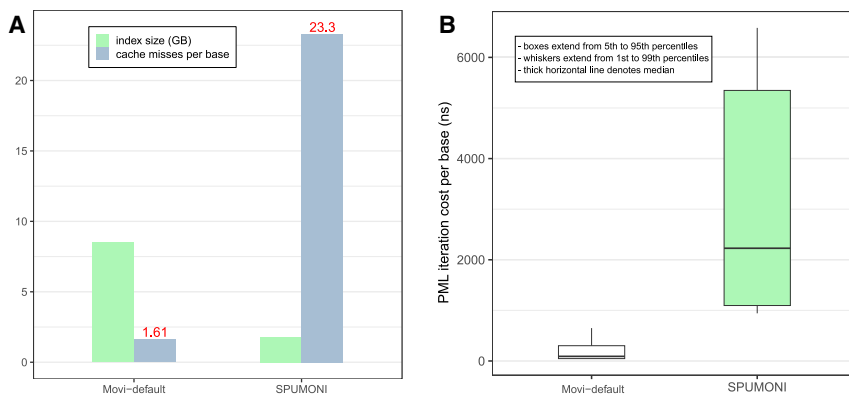


**Figure 3. Comparisons of Movi-default and SPUMONI in terms of query speed and predictability**

(A) Index size and cache miss rate for Movi and SPUMONI. The better cache miss rate in Movi is the result of locality of the reference in move structure. (B) Time for computing PMLs per base. Boxes extend from 5th to 95th percentiles and whiskers extend from 1<sup>th</sup> to 99<sup>th</sup>. Thick horizontal line denotes median.

Fulgor had both a smaller index and a relatively fast query time compared even to Movi, taking only about 3.8 times the amount of time as Movi-default. Fulgor's full index takes about 3 GB, about one-third the size of Movi-default's 8.5 GB index. On the other hand, the two tools output different results, with Movi outputting pseudo-matching lengths and Fulgor outputting pseudo-alignment information. Further, Fulgor is k-mer based and requires pre-selection of a set k-mer length, whereas Movi is a full-text index. Movi-default is the fastest overall and provides an advantageous trade for applications that benefit from the flexibility of a full-text index, e.g., adaptive sampling.

Bowtie2 and minimap2 are not perfectly comparable to Movi since they produce full read alignments. Further Bowtie2 is designed for use with short reads, not the long nanopore reads assessed here. For that reason, we omitted Bowtie2 from the speed comparison. Minimap2 took about 69 times longer to align the reads, while also using 16 threads (compared to 1 thread for the other tools). Its index was also eight times larger than Movi-default's. So although minimap2 is able to produce full and accurate alignments for the nanopore reads (Movi only computes the pseudo matching lengths), Movi provides a useful combination of speed and memory efficiency for applications, such as classification, where pseudo-matching lengths provide sufficient power.

Finally, we compared the PMLs generated by Movi (both modes) against those computed by SPUMONI. Using the diff tool, we found that Movi and SPUMONI generated identical PMLs, as expected.

### Speed and predictability of Movi queries

Because of its simple tabular form, we hypothesized the move structure would exhibit superior cache characteristics compared to SPUMONI. We used the "Cachegrind" profiler to measure the cache misses incurred by Movi and SPUMONI when computing PMLs for the same Zymo sample used in the previous section. Specifically, we measured misses in the "last-level" cache, i.e., the final level of cache before main memory, since these are the misses that take the most time.

Figure 3A shows the number of cache misses per base. We observed that SPUMONI incurred more than 14 times as many cache misses per base compared to Movi. The reduced cache miss rate of Movi came at the cost of a larger index. We also observed that the time required for each iteration of the inner

loop was both smaller and less variable for Movi compared to SPUMONI.

To assess the latencies of LF-mapping executed by SPUMONI and Movi more precisely, we employed the chrono high-resolution clock in C++ to make nanosecond-level latency measurements for their inner loops. The distribution of these latencies is visualized as boxplots in Figure 3B. We observed that iterations of the Movi inner loop were about 11.5 times faster than those of SPUMONI (comparing means). The 99th-percentile latency observed for Movi's inner loop (650 ns) was smaller than the 1st-percentile latency observed for SPUMONI's inner loop (942 ns). The median latency observed for Movi's inner loop (91 ns) was also much smaller than SPUMONI's (2,228 ns). Note that a single last-level cache miss is roughly thought to take 100 ns or 300 clock cycles on a 3 GHz processor.

Besides variability in inner loop performance due to cache misses, we measured the number of fast-forward iterations and repositioning scans in each of Movi's modes. These were discussed in Sec. Computing pseudo matching lengths. As expected, the number of operations was bounded by a small constant for Movi-constant. For Movi-default, the number of operations varied much more, as seen in Figure 4. Detailed statistics are presented in supplementary materials Table S4. Although earlier we observed that Movi-default was faster than Movi-constant on average, here we saw that Movi-constant's inner loop performed a smaller and more predictable number of operations, which is advantageous in situations where the algorithm must keep up with the output of an instrument in real-time. However, the average number of fast-forwards performed in Movi-default's loop compared to Movi-constant's was only about 1.2 times greater, and the average number of repositioning scans was only about 2.5 times greater. The fact that Movi-default is still faster than Movi-constant despite this difference is likely because Movi-constant requires a larger index, which in turns incurs more cache misses overall.

### Extrapolation to nanopore throughputs

Using per-base speeds measured for the Zymo input data (presented in Table 2), we extrapolate to measure their ability to analyze nanopore sequencing data in a real-time adaptive sampling context. We assume that the sequences are base-called immediately. Considering that the sequencing speed of each nanopore of an Oxford Nanopore (ONT) instrument is 420 base pairs per second, SPUMONI's speed is sufficient to

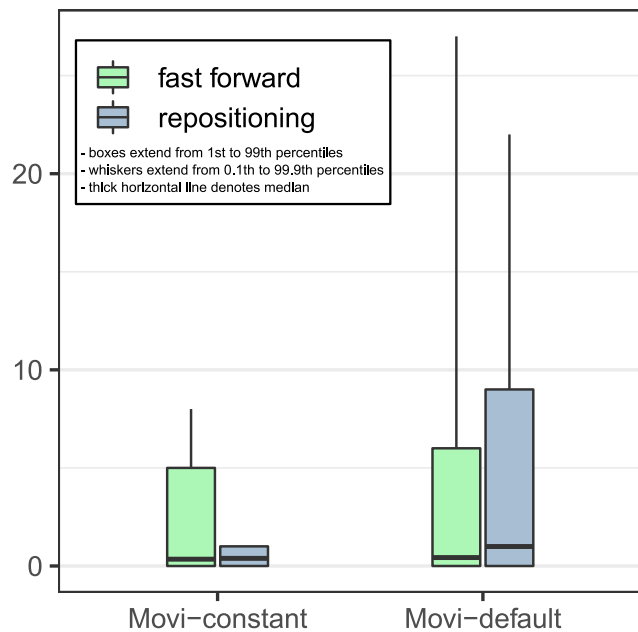


**Figure 4. The number of fast-forwards and repositioning scans in each mode of Movi**

Movi-constant is guaranteed to use a constant number of memory accesses per LF-mapping. Boxes extend from 1st to 99th percentiles and whiskers extend from 0.1<sup>th</sup> to 99.9<sup>th</sup>. Horizontal line denotes mean. In all cases, the median is 0.

simultaneously handle 904 channels (pores) at once. On the other hand, Movi can handle 26,890 simultaneous channels, surpassing the total number of channels in the largest flow cell available for the PromethION device: 2,675 channels (Accessed October 4, 2023. <https://nanoporetech.com/products/specifications>). Assuming perfect linear scaling, about five simultaneous Movi threads (each handling 16 reads concurrently) would be sufficient to handle the aggregate output of 48 PromethION flowcells.

#### Backward search for count queries

Besides pseudo-matching lengths, another full-text query is the “count” query, which reports the number of distinct locations where the query occurs as a substring of T. A count query involves a sequence of backward-search steps, each step using one additional character of the query.

In Movi, backward search begins by finding the range of BWM rows that have the final (rightmost) query character as a prefix. In subsequent steps, LF-mapping-like steps are used to advance this range’s top and bottom pointers to additionally match the next query character to the left (i.e., a longer suffix of the query), obtaining an interval of BWM rows beginning with the longer suffix. This repeats until the query is exhausted or until the range becomes empty, indicating that the query does not occur. In Movi, updating the top and bottom pointers is exactly analogous to the repositioning procedure described in Methods [Computing pseudo matching lengths](#), except that the choice of  $j^{up}$  or  $j^{dn}$  is determined by whether we are updating the top pointer (in which case we use  $j^{dn}$ ) or the bottom pointer (in which case we use  $j^{up}$ ).

**Table 3. Time and index size required to execute the count query with Movi and the r-index**

Mode	Index size (GB)	Query time (mm:ss)	Speedup
r-index	1	44:05	1 ×
Movi-default	3.2	2:43	16.2 ×
Movi-constant	11	2:48	15.7 ×

Both default and constant modes of Movi are very fast, whereas the constant mode uses more memory, because it stores the repositioning pointers in each row.

To measure backward search performance, we used Mason<sup>15</sup> to simulate 10 million 150-bp unpaired reads from an FASTA file containing the complete genomes of the seven bacterial species in the Zymo community, which was also used for [Results Sec. Pseudo matching lengths](#) for a mock community. We generated error-free reads to ensure that backward search would iterate over all query characters. We compared Movi’s efficiency to that of r-index, which supports the same query. Note that SPUMONI does not support this same query. The results are presented in [Table 3](#). We observed that r-index took 44m:05s, whereas Movi took 2m:43s, a 16-fold improvement. On the other hand, the Movi-default index was about three times larger than the r-index, consistent with other results showing the move structure to be larger.

#### Scaling to human pangenomes

We next evaluated the scalability of Movi using human genome haplotype assemblies from the Human PanGenome Reference Consortium (HPRC).<sup>12</sup> We selected various numbers of haplotypes, ranging from 1 to 94, which includes all available haplotypes. We measured the overall size and scalability of Movi’s indexes (based on the move structure) when compared to SPUMONI (based on r-index) and Fulgor (based on colored compacted De Bruijn graph). Note that Fulgor’s index also stores “color” information (associating k-mers with haplotypes), which is not a type of information stored in the Movi or SPUMONI indexes. We used  $k = 31$  and  $m = 19$  when building the Fulgor indexes.

We measured each tools’ ability to scale to larger pangenomes in [Table 4](#). As a baseline for measuring scalability, we reported the number of distinct k-mers in the input according to Fulgor’s stats command (“kmer-count” column). As a second baseline, we also reported the number of runs in the BWT according to Movi (“r” column). As seen in [Figure 5](#), the size of the 94-haplotype indexes was less than two times the size of the 5-haplotype indexes for all three tools. Movi exhibited the best scaling factor, with its 94-haplotype index using about 1.2 times the space as its 5-haplotype index. The 94-haplotype index for Fulgor and SPUMONI used 1.38 and 1.86 times the space as their 5-haplotype indexes, respectively. This highlights the advantages of compressed indexes, including full-text indexes, when indexing large pangenomes.

We also observed that the size of Fulgor’s index was considerably smaller than both SPUMONI’s and Movi’s. Fulgor’s index includes both k-mer mapping and color class information, i.e.,

**Table 4. Indexes are built over different number of HPRC assemblies: 1, 5, 10, 25, 50, 75, 94 (all)**

Reference	FASTA (GB)	kmer-count (x10 <sup>9</sup> )	Fulgor(GB)	r (x10 <sup>9</sup> )	SPUMONI (GB)	Movi(GB)
HPRC 1	2.9	2.50	3.1	3.33	6	62
HPRC 5	15	2.70	3.7	3.53	8.6	66
HPRC 10	29	2.79	3.9	3.65	9.8	68
HPRC 25	74	2.94	4.3	3.84	13	72
HPRC 50	174	3.06	4.7	4.02	14	75
HPRC 75	214	3.13	4.9	4.14	15	78
HPRC 94	268	3.19	5.1	4.24	16	79

For Movi and SPUMONI, the index contains both the forward and reverse complement strands of the haplotypes.

information about which k-mers occur in which haplotypes. In this experiment, there are relatively few colors, and so color-class information makes up a smaller portion of the index. Running Fulgor’s “stats” command on indexes created in Table 4 showed that between 1% and 5% of the index is dedicated to color information.

We also evaluated query speed for each tool using a simulated long read sample and a “combined” sample, consisting of both simulated reads and real reads from a human gut microbiome sample.<sup>16</sup> This allows us to measure performance in a scenario where many input reads do not have a long match to the reference pangenome. The results are shown in supplementary materials Table S5, and a similar trend as in Sec. Pseudo matching lengths for a mock community is observed, with Movi being the fastest followed by Fulgor and SPUMONI. Movi is 1.7x to 2.7x faster than Fulgor and 23x to 27x faster than SPUMONI in all

the experiments with either a single human genome or the human pangenome.

## DISCUSSION

We introduced Movi, a cache-efficient, scalable tool for pangenomic indexing and read classification. Movi’s index is based on the move structure, which is a full-text index with a scaling factor superior to competing approaches like SPUMONI and Fulgor. Movi is extremely fast, due both to its excellent locality of reference that in turn minimizes cache misses and to our novel strategy for hiding the remaining cache-miss latency by processing many reads concurrently. Movi’s rapid and predictable query speed makes it well suited to applications like nanopore adaptive sampling. Movi can process the base-called output of a fully loaded PromethION using 12 threads.

The move structure’s simple tabular structure suggests simple ways to partition and distribute it across nodes of a computer cluster while minimizing inter-node communication. It can simply be divided into separate, contiguous chunks of rows, which can then be distributed. Execution of a pattern-matching query will require some jumps between nodes (i.e., a longer-distance LF query) but will frequently require only sequential or nearby jumps (fast-forwards and repositions) that do not require moving across nodes. This provides a much more favorable substrate for distributed computing compared to r-index, which is characterized by complex and unpredictable memory accesses.

Another key advantage of our full-text indexing approach is that it does not require the user to select any key parameters ahead of time. This is in contrast to k-mer-based or minimizer-based approaches, for which the user must be aware of the potential pitfalls of choosing suboptimal parameters.

## Limitations of the study

A limitation of Movi is the fact that the M table is large compared to all the other tools assessed here (besides minimap2). Movi’s index uses a table with  $O(r)$  rows, where each row explicitly stores the LF-mapping result for the run head, requiring  $O(\log(r))$  bits to point to another row. This approach leads to a larger overall table size compared to the r-index, which uses bit-vectors and other structures that, although they have poor locality of reference, tend to reduce the number of bits stored per run. In the future, it will be important to reduce the footprint of Movi’s index. This could be accomplished, for instance, by adopting the

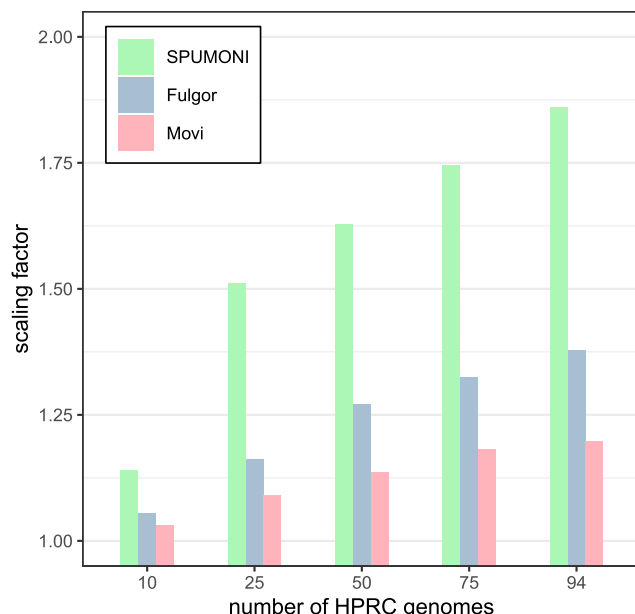


**Figure 5. The scaling factor is computed by dividing the size of each tool’s index by the size of the index of that tool built over five HPRC genomes**

All tools have small scaling factors for pangenomes. While Movi’s index is the largest compared to the other two, it has the best scaling factor for any number of hpc genomes.

minimizer digestion strategy of SPUMONI 2.<sup>6</sup> Another space-saving measure could be to losslessly compress the move structure using, e.g., the columnar compression strategies investigated by Brown et al. in 2022.<sup>11</sup>

We also hope to expand Movi's applicability to more query types. For instance, Movi could be adapted to handle multi-class classification by augmenting the index with suffix array or "document" information.<sup>17</sup>

Although Fulgor<sup>18</sup> optimizes space and time by capitalizing on long unitigs and explicitly storing the corresponding strings, we can adopt a similar strategy by leveraging substructures within the BWT. One such approach is to enhance query efficiency by reordering the BWT rows. This technique can be seamlessly integrated into Movi, enabling further cache efficiency and greater speed. By incorporating reordering, Movi has the potential to achieve even greater query performance.

## RESOURCE AVAILABILITY

### Lead contact

Further information and requests for resources should be directed to and will be fulfilled by the lead contact, Ben Langmead ([langmea@cs.jhu.edu](mailto:langmea@cs.jhu.edu)).

### Materials availability

This study did not generate any new materials.

### Data and code availability

- Data: For the Mock Community experiment, we used the SRA project under the accession number SRX7711546. We obtained bacterial reference genomes from NCBI. The list of the references are available at: <https://github.com/mohsenzakeri/Movi-experiments/blob/main/zymo/refs/bacteria.txt>.  
The human pangenome was obtained from the Human Pangenome Reference Consortium website: <https://humanpangenome.org/>  
The human gut microbiome sample was downloaded from the SRA under the accession number SRR9847854. The simulated human reads were generated by PBSIM2<sup>19</sup> using the R9.4 chemistry. The CHM13 human genome<sup>20</sup> was used for simulating the reads.
- Code: Movi is implemented in C++. It is GPL3-licensed open-source software available from <https://github.com/mohsenzakeri/movi>.  
Movi uses the prefix-free parsing implementation from the pfp\_thresholds repository at <https://github.com/maxrossi91/pfp-thresholds> for building the Burrows Wheeler Transform of the pangenome.  
Movi uses the run splitting implementation from the r-permute library at <https://github.com/drnatebrown/r-permute>.
- Others: Cachegrind was used for evaluating the number of cache misses. It is part of Valgrind software and was obtained from: <https://valgrind.org/docs/manual/cg-manual.html>.

## ACKNOWLEDGMENTS

This work was supported by NIH grants R01HG011392 and R21HG013433, and NSF-135491 awarded to B.L. N.K.B. and T.G. were supported by NSERC grant RGPIN-07185-2020 to T.G. N.K.B. was also supported by a Johns Hopkins University Computer Science PhD Fellowship.

## AUTHOR CONTRIBUTIONS

M.Z. and B.L. designed the method, with help from N.K.B., O.Y.A., and T.G. M.Z. wrote the software with help from N.K.B. M.Z. performed the experiments. All authors contributed to the manuscript.

## DECLARATION OF INTERESTS

B.L. is the owner of InOrder Labs LLC.

## STAR★METHODS

Detailed methods are provided in the online version of this paper and include the following:

- KEY RESOURCES TABLE
- METHOD DETAILS
  - Burrows Wheeler Transform, FM-index and r-index
  - TheMoveDataStructure
  - Computing pseudo matching lengths
  - Cache-miss latency hiding
  - The Movi software
- QUANTIFICATION AND STATISTICAL ANALYSIS

## SUPPLEMENTAL INFORMATION

Supplemental information can be found online at <https://doi.org/10.1016/j.isci.2024.111464>.

Received: September 7, 2024

Revised: October 11, 2024

Accepted: November 20, 2024

Published: November 27, 2024

## REFERENCES

1. Wood, D.E., and Salzberg, S.L. (2014). Kraken: ultrafast metagenomic sequence classification using exact alignments. *Genome Biol.* 15, 1–12. <https://doi.org/10.1186/gb-2014-15-3-r46>.
2. Wood, D.E., Lu, J., and Langmead, B. (2019). Improved metagenomic analysis with Kraken 2. *Genome Biol.* 20, 257. <https://doi.org/10.1186/s13059-019-1891-0>.
3. Kim, D., Song, L., Breitwieser, F.P., and Salzberg, S.L. (2016). Centrifuge: rapid and sensitive classification of metagenomic sequences. *Genome Res.* 26, 1721–1729. <https://doi.org/10.1101/gr.210641.116>.
4. Menzel, P., Ng, K.L., and Krogh, A. (2016). Fast and sensitive taxonomic classification for metagenomics with Kaiju. *Nat. Commun.* 7, 11257. <https://doi.org/10.1038/ncomms11257>.
5. Ahmed, O., Rossi, M., Kovaka, S., Schatz, M.C., Gagie, T., Boucher, C., and Langmead, B. (2021). Pan-genomic matching statistics for targeted nanopore sequencing. *iScience* 24, 102696. <https://doi.org/10.1016/j.isci.2021.102696>.
6. Ahmed, O.Y., Rossi, M., Gagie, T., Boucher, C., and Langmead, B. (2023). Spumoni 2: improved classification using a pangenome index of minimizer digests. *Genome Biol.* 24, 122. <https://doi.org/10.1186/s13059-023-02958-1>.
7. Ferragina, P., and Manzini, G. (2005). Indexing compressed text. *J. ACM* 52, 552–581. <https://doi.org/10.1145/1082036.1082039>.
8. Gagie, T., Navarro, G., and Prezza, N. (2018). Optimal-time text indexing in bwt-runs bounded space. In *Proceedings of the Twenty-Ninth Annual ACM-SIAM Symposium on Discrete Algorithms (SIAM)*, pp. 1459–1477. <https://doi.org/10.1137/1.9781611975031.96>.
9. Rossi, M., Oliva, M., Langmead, B., Gagie, T., and Boucher, C. (2022). MONI: A Pangenomic Index for Finding Maximal Exact Matches. *J. Comput. Biol.* 29, 169–187. <https://doi.org/10.1089/cmb.2021.0290>.
10. Nishimoto, T., and Tabei, Y. (2021). Optimal-time queries on bwt-runs compressed indexes. In *48th International Colloquium on Automata, Languages, and Programming (ICALP 2021)*, 198, p. 101, (Schloss Dagstuhl-Leibniz-Zentrum für Informatik). <https://doi.org/10.4230/LIPIcs.ICALP.2021.101>.

11. Brown, N.K., Gagie, T., and Rossi, M. (2022). RLBWT Tricks. In 20th International Symposium on Experimental Algorithms (SEA 2022), Vol. 233 of Leibniz International Proceedings in Informatics (LIPIcs), 16, C. Schulz and B. Uçar, eds., pp. 1–16:16, (Schloss Dagstuhl – Leibniz-Zentrum für Informatik, Dagstuhl, Germany, 2022). <https://doi.org/10.4230/LIPIcs-SEA.2022.16>.
12. Liao, W.-W., Asri, M., Ebler, J., Doerr, D., Haukness, M., Hickey, G., Lu, S., Lucas, J.K., Monlong, J., Abel, H.J., et al. (2023). A draft human pangenome reference. *Nature* 617, 312–324. <https://doi.org/10.1038/s41586-023-05896-x>.
13. Kovaka, S., Fan, Y., Ni, B., Timp, W., and Schatz, M.C. (2021). Targeted nanopore sequencing by real-time mapping of raw electrical signal with uncalled. *Nat. Biotechnol.* 39, 431–441. <https://doi.org/10.1038/s41587-020-0731-9>.
14. O'Leary, N.A., Wright, M.W., Brister, J.R., Ciuffo, S., Haddad, D., McVeigh, R., Rajput, B., Robbertse, B., Smith-White, B., Ako-Adjei, D., et al. (2016). Reference sequence (refseq) database at ncbi: current status, taxonomic expansion, and functional annotation. *Nucleic Acids Res.* 44, D733–D745. <https://doi.org/10.1093/nar/gkv1189>.
15. Holtgrewe, M. (2010). Mason-a read simulator for second generation sequencing data. Technical Report FU Berlin. <http://publications.imp.fu-berlin.de/962/>.
16. Moss, E.L., Maghini, D.G., and Bhatt, A.S. (2020). Complete, closed bacterial genomes from microbiomes using nanopore sequencing. *Nat. Biotechnol.* 38, 701–707. <https://doi.org/10.1038/s41587-020-0422-6>.
17. Ahmed, O., Rossi, M., Boucher, C., and Langmead, B. (2023). Efficient taxa identification using a pangenome index. *Genome Res.* 33, 1069–1077. <https://doi.org/10.1101/gr.277642.123>.
18. Fan, J., Khan, J., Singh, N.P., Pibiri, G.E., and Patro, R. (2024). Fulgor: a fast and compact k-mer index for large-scale matching and color queries. *Algorithm Mol. Biol.* 19, 3. <https://doi.org/10.1186/s13015-024-00251-9>.
19. Ono, Y., Asai, K., and Hamada, M. (2021). Pbsim2: a simulator for long-read sequencers with a novel generative model of quality scores. *Bioinformatics* 37, 589–595. <https://doi.org/10.1093/bioinformatics/btaa835>.
20. Nurk, S., Koren, S., Rhie, A., Rautiainen, M., Bzikadze, A.V., Mikheenko, A., Vollger, M.R., Altemose, N., Uralsky, L., Gershman, A., et al. (2022). The complete sequence of a human genome. *Science* 376, 44–53. <https://doi.org/10.1126/science.abj6987>.
21. Brown, N. (2023). Bwt-runs compressed data structures for pan-genomics text indexing. <http://hdl.handle.net/10222/82419>.
22. Bannai, H., Gagie, T., and Tomohiro, I. (2020). Refining the *r*-index. *Theor. Comput. Sci.* 812, 96–108. <https://doi.org/10.1016/j.tcs.2019.08.005>.
23. Anderson, T., and Wheeler, T.J. (2021). An optimized fm-index library for nucleotide and amino acid search. *Algorithm Mol. Biol.* 16, 25. <https://doi.org/10.1186/s13015-021-00204-6>.
24. Boucher, C., Gagie, T., Kuhnle, A., Langmead, B., Manzini, G., and Mun, T. (2019). Prefix-free parsing for building big bwts. *Algorithm Mol. Biol.* 14, 13–15. <https://doi.org/10.1186/s13015-019-0148-5>.

## STAR★METHODS

## KEY RESOURCES TABLE

REAGENT or RESOURCE	SOURCE	IDENTIFIER
<b>Deposited data</b>		
ZymoMC sequencing reads	Kovaka et al. <sup>13</sup>	<a href="https://www.ncbi.nlm.nih.gov/sra/SRX7711546">https://www.ncbi.nlm.nih.gov/sra/SRX7711546</a>
Human pangenome reference (HPRC)	Liao et al. <sup>12</sup>	<a href="https://www.nature.com/articles/s41586-023-05896-x">https://www.nature.com/articles/s41586-023-05896-x</a>
Human gut metagenome reads	Moss et al. <sup>16</sup>	<a href="https://www.ncbi.nlm.nih.gov/sra/?term=SRR9847854">https://www.ncbi.nlm.nih.gov/sra/?term=SRR9847854</a>
Telomere-to-Telemere Consortium CHM13 v1.0 assembly	Nurk et al. <sup>20</sup>	<a href="https://github.com/marbl/CHM13">https://github.com/marbl/CHM13</a>
<b>Software and algorithms</b>		
Movi	This paper	<a href="https://github.com/mohsenzakeri/Movi">https://github.com/mohsenzakeri/Movi</a>
PBSIM2	Ono et al. <sup>19</sup>	<a href="https://github.com/yukiteruono/pbsim2">https://github.com/yukiteruono/pbsim2</a>
Mason	Holtgrew <sup>15</sup>	<a href="https://www.seqan.de/apps/mason.html">https://www.seqan.de/apps/mason.html</a>

## METHOD DETAILS

## Burrows Wheeler Transform, FM-index and r-index

The Burrows Wheeler Transform (BWT) is a reversible permutation that reorders the characters of a string  $T$  according to the lexicographical order of their right contexts in  $T$ . Beginning with  $T$  of length  $n$ , we append a terminal symbol  $\$$  that does not appear elsewhere in  $T$  and is lexicographically smaller than  $T$ 's other characters.  $T[i]$  denotes the character at 1-based offset  $i$  and  $T[i..n]$  denotes a suffix starting at  $i$ .  $BWT(T)$  permutes  $T$ 's characters so that  $T[i]$  comes before  $T[j]$  in BWT order if and only if  $T[i+1..n] < T[j+1..n]$ . Repetitive portions of  $T$  yield long “runs” in  $BWT(T)$  where a run is a maximal-length substring consisting of a character repeated. Figure 1A illustrates BWT runs of length up to 8 in the last column of the matrix.

Figures 1A and 1B show two copies of a Burrows-Wheeler Matrix or BWM. Rows of the BWM consist of all distinct rotations of the string  $T$  ordered lexicographically.  $BWT(T)$  is the last column of  $BWM(T)$ . BWM's first and last columns are related by the Last-to-First mapping (“LF-mapping”),<sup>7</sup> which states that the  $i^{\text{th}}$  occurrence of a character  $c$  in the last column of the BWM corresponds to the same text occurrence as the  $i^{\text{th}}$  occurrence of  $c$  in the first column. Some LF-mapping relationships are illustrated with parallelograms in Figure 1A. The LF-mapping also gives a way to navigate through the text  $T$ . Note that if the BWT permutation maps  $T[j]$  to  $BWT[i]$ , then  $LF[i]$  gives the BWT index of  $T[j-1]$  (or  $T[n]$  if  $j = 1$ ). So the LF-mapping allows for right-to-left movements with respect to  $T$ , a fact used in pattern-matching queries.

The FM-index is a data structure based on  $BWT(T)$  enabling fast and efficient computation of the LF-mapping and related queries. It consists of  $BWT(T)$  as well as succinct data structures for storing and querying character ranks within  $BWT(T)$ . In typical implementations, it grows linearly with the text:  $O(n)$ .

When  $T$  is repetitive, the number of BWT runs ( $r$ ) is much smaller than the text length ( $n$ ). The r-index<sup>8</sup> exploits this by representing the BWT in a run-length-compressed fashion. This version is called the RLBWT. The  $i^{\text{th}}$  run, denoted  $RLBWT[i]$ , consists of the character repeated in the run ( $RLBWT[i].c$ ), and the run's length ( $RLBWT[i].n$ ). Additional data structures enable efficient computation of the LF-mapping without having to decompress the RLBWT. The data structures making up the r-index fit in  $O(r)$  space total.

As a brief demonstration of how  $r$  grows with a typical pangenome, we measured number of runs in the BWT for an increasing proportion of bacterial genomes in Table 1. The number of runs for an increasing number of complete *Salmonella* genomes from 1 to 1550 is also displayed in supplementary materials Table S1. The number of runs ( $r$ ) increases at a slower rate compared to the total length of the reference ( $n$ ). The value  $\frac{n}{r}$  represents a rough compression ratio. As a complementary measure, we also report the number of distinct canonical k-mers ( $k = 31$ ) present, which grows similarly to the number of BWT runs.

## TheMoveDataStructure

## LF mapping

When  $T$  is a repetitive pangenome, the LF-mapping tends to map consecutive stretches of BWT characters to consecutive stretches in  $F$  (Figure 1A). The move structure exploits this to simplify computation of the LF-mapping. The move structure consists of a table ( $M$ ) with rows corresponding to BWT runs (Figure 1C). To aid LF-mapping, the column named  $\pi$  stores the LF-mapping of the run head, i.e.,  $M[i].\pi = LF[M[i].p]$ . To compute the LF-mapping at any offset in run index  $i$ , we begin by following  $M[i].\pi$ . This will either jump to the correct run, or to a run preceding the correct one.

Given  $M$ , a BWT offset  $j$ , and a run index  $i$ , we compute  $LF[j]$  by adding  $j$ 's offset into the current run ( $j - M[i].p$ ) to the run head's LF-mapping:

$$LF[j] = M[i].\pi + (j - M[i].p)$$

Note that this involves only arithmetic on  $i$ ,  $j$ ,  $M[i.\pi]$  and  $M[i.p]$ , and does not involve bitvectors or wavelet-tree queries. Only the accesses to  $M[i]$  might require accessing main memory. An illustration of how memory accesses induced by move structure queries differ than those by r-index is shown in supplementary materials [Figure S4](#).

Note that an input to this computation is  $i$ , the current run index. To chain multiple LF-mapping queries together, as is needed for matching queries, we must update not only the BWT offset  $j$  but also the BWT run index  $i$ . As a step toward this goal,  $M[i.\xi]$  stores the index of the run containing  $LF[M[i.p]]$ . However, the run containing  $LF[M[i.p]]$  may not also contain  $LF[j]$ . I.e. it is possible that  $LF[j] \neq M[M[i.\xi].p] > M[M[i.\xi].\ell]$ . After jumping to  $M[M[i.\xi].\ell]$ , we may additionally need to advance through the runs until finding the smallest run index  $i' > i$  such that  $M[i'.p] \leq LF[j] < M[i'+1.p]$ . We call this the “fast-forward” or “ff” procedure, illustrated in [Figure 1B](#) (top) and detailed by [Data S1](#) in supplementary materials. Using that algorithm, we update both  $i$  and  $j$  in each LF-mapping step:

$$i' \leftarrow ff(M, i, j) \quad j' \leftarrow M[i.\pi] + (j - M[i.p])$$

### Constant-time LF

Nishimoto and Tabei gave a procedure for splitting some BWT runs into shorter sub-runs to achieve a constant upper bound on the fast-forwards required for any LF-mapping.<sup>10</sup> The procedure works with a parameter  $d$  such that, after splitting runs, the number of fast-forwards per LF-mapping query is less than  $2d$  while adding at most  $\frac{r}{d-1}$  additional runs to the table. The overall number of runs is still  $O(r)$  after splitting. In practice, the procedure splits only a fraction of the original runs.<sup>21</sup>

With the exception of the jump induced by following  $M[i.\xi] = LF[M[i.p]]$ , all the memory accesses described here are sequential. The  $LF[M[i.p]]$  step is unpredictable, possibly needing to access a distant and not-recently-accessed location in memory, likely incurring a cache miss. That said, for a chain of several LF-mapping queries, only one expensive memory access is needed per query.

Since information about exact BWT offsets of matches is not required for computing pseudo matching lengths, Movi avoids storing both  $p$  and  $\pi$  in the table. Instead, Movi collapses those fields into a single relative offset, as previously implemented by Brown et al.<sup>11</sup>

### Computing pseudo matching lengths

#### Matching statistics and pseudo matching lengths

Matching statistics (MS) are a summary of sequence similarity used in sequence classification tasks and for computing other similarity features like Maximal Exact Matches (MEMs). Given a text  $T[1..n]$  and pattern  $P[1..m]$ ,  $P$ ’s matching statistics with respect to  $T$  are defined as an array  $MS[1..m]$  where  $MS[i]$  is the length of the longest prefix of  $P[i..m]$  occurring in  $T$ .

Bannai et al.<sup>22</sup> described a 2-pass procedure for computing matching statistics using the r-index and an auxiliary thresholds structure. Rossi et al.<sup>9</sup> gave an efficient procedure for computing the thresholds. Later, Ahmed et al.<sup>5</sup> introduced a modified 1-pass version of the procedure that computes a vector of Pseudo Matching Lengths (PMLs), which roughly approximate the lengths in MS. While PMLs contain less information than MSs – e.g., they cannot be used to exactly compute MEMs – finding PMLs is much faster, can be performed in single pass over the query, and requires neither a suffix-array sample nor a random-access structure for  $T$ . In practice, PMLs are similar to MSs in their ability to classify sequences.<sup>5</sup>

The MONI algorithm starts at an arbitrary offset in the BWT, then considers each character of the query sequence in right-to-left order. Say we are currently at offset  $j$  in BWT and are examining character  $P[i]$ . The algorithm first tests if  $P[i] = BWT[j]$ . If they are equal, we call this “case 1.” For case 1, the algorithm performs an LF-mapping step and moves on to the next character:

$$i' \leftarrow i - 1 \quad j' \leftarrow LF[j]$$

The LF-mapping uses the strategy we discussed above, which includes the fast-forward procedure. If  $P[i] \neq BWT[j]$ , we call this “case 2.” For case 2, we cannot simply use  $LF[j]$  as our next offset; rather we must “reposition” to a nearby offset  $j'$  such that  $P[i] = BWT[j']$ . We let  $j'$  equal one of two choices: the greatest  $j^{up}$  such that  $j^{up} < j$  and  $BWT[j^{up}] = P[i]$ , or the smallest  $j^{dn}$  such that  $j^{dn} > j$  and  $BWT[j^{dn}] = P[i]$ . Whether we choose  $j^{up}$  or  $j^{dn}$  is determined by querying the thresholds structure of Bannai et al.<sup>22</sup> Movi stores the thresholds structure as additional columns in the move structure. If  $\sigma$  is the number of characters in the alphabet, e.g., 4 for DNA sequences,  $\sigma - 1$  thresholds are stored in each row of the table to be able to reposition based on the character observed in the query. Once we have repositioned, we proceed using the same update rule as above, substituting  $j'$  for  $j$ .

Instances where we can apply the simpler case 1 update rule correspond to instances where an existing match is being extended by 1 character, causing the matching statistic to increase by one. Instances where we apply case 2 might or might not correspond to an extension. The MS algorithm from MONI is capable of distinguishing these two subcases of case 2. The PML algorithm of SPUMONI is not capable of this, instead resetting the match length to 0 when it reaches an instance of case 2. Details about the PML computation procedure is shown by [Data S2](#) in supplementary materials.

#### Movi’s repositioning

Movi uses two distinct strategies for finding and moving to the run containing  $j'$ . By default, Movi scans from run to run (either upward to  $j^{up}$  or downward to  $j^{dn}$ ) until reaching a run with a matching character. This involves an unpredictable number of memory accesses, though they are sequential accesses. In its Movi-constant mode (discussed further in Methods 12.5), Movi instead stores explicit pointers to the  $j'$ -containing runs for each characters of the DNA alphabet. It stores two such sets of pointers, one for when the threshold points upward and one for when it points downward, leading to a total of six additional pointers being stored in each move structure run.

In short, there are three types of operations performed by Movi during the PML computation: (1) jump to the run potentially containing the LF-mapping destination, (2) fast-forward to the run that contains the LF-mapping destination, and (3) reposition to the run containing a matching character in the case of a mismatch. These are illustrated in a state diagram in [Figure 2](#) (with further detail in supplementary materials [Figure S1](#)). Operation (1) is used in each LF-mapping, once per base, and has the highest cost since it usually incurs a cache miss. Operations (2) and (3) are less expensive.

### Cache-miss latency hiding

The once-per-iteration LF-mapping step is Movi's single most expensive operation. Because it moves to a new, unpredictable address, it usually incurs a cache miss and thereby stalls the processor until the requested memory (and associated cache line) is retrieved and installed in the cache. AWFM-index,<sup>23</sup> a lightweight FM index library optimized for genomic sequences, uses manual prefetching to improve memory access latency, but the authors reported that the strategy was not effective.

We observed that Movi's simple inner loop can be easily rearranged and augmented with memory "prefetch" instructions in a way that avoids the latency of stalling. To achieve this, a single thread of execution processes several reads concurrently. Say that Movi is computing PMLs for two reads named `read_a` and `read_b` concurrently in a single thread. Rather than compute all of `read_a`'s PMLs then all of `read_b`'s PMLs, Movi alternates repeatedly between the reads. It first advances the computation for `read_a` until reaching the first instruction that accesses memory in the LF-mapping step's destination row. Instead of attempting the access immediately, Movi issues a memory prefetch instruction, which asynchronously requests that the needed memory be retrieved into the cache. Because this happens asynchronously, it does not immediately cause the processor to stall. Movi then switches to `read_b` and advances that computation in a similar way, ending with the prefetch of the destination row of `read_b`'s next LF-mapping step. Movi then switches back to `read_a`; in the meantime, the processor has at least begun (and has possibly completed) the process of installing the earlier-requested memory into the cache. We now resume the computation for `read_a`, expecting that accessing the destination row of the LF-mapping can now be done with little or no stalling. This process repeats until all the PMLs are computed for both reads. We give an illustration in supplementary materials [Figure S2](#) for the strategy, the pseudocode is also provided in supplementary materials [Data S3](#). Note that the pseudocode handles various special cases of interest, e.g., detecting when a read's sequence has been exhausted and loading the next read.

Based on the cache latency of the machine, this "latency hiding" strategy depends on a parameter: the number of reads handled concurrently. If too few reads are handled concurrently, only a fraction of the stalling time is avoided and the benefit is small. If too many reads are handled concurrently, the time between the prefetch and the actual use of the memory can become so long that competing threads and processes have caused the cache line to be erased ("evicted") from the cache, and the stall occurs anyway. We measured the speed of Movi's PML computation when using 2, 4, 8, 16, and 32 concurrent reads. Once reaching about 8 concurrent reads, the gain from prefetching began to plateau supplementary materials [Figure S3](#). We therefore chose 16 as the default number of concurrent reads, and that setting is used in all results in the manuscript. Use of 16 concurrent reads improved throughput 2.24-fold compared to when latency hiding was disabled.

### The Movi software

Movi supports two modes of operation. The first mode, called Movi-default, is fast but lacks the constant-time LF-mapping query guarantee. The second mode, called Movi-constant, uses the splitting to create a move structure that has a constant-time LF-mapping guarantee. Further, Movi-constant uses a constant-time version of the repositioning step, allowing its inner loop to be fully constant-time, regardless of whether it involves LF-mapping steps and/or repositioning. This comes at the cost of additional space, since (a) the move structure that results from the splitting procedure has more runs and is therefore somewhat larger than the unsplit move structure, and (b) the constant-time repositioning step requires that we pre-compute upward and downward jump distances and store them in the move structure table.

To build the Burrows Wheeler Transform, Movi uses the prefix-free parsing (PFP) algorithm of Boucher et al.,<sup>24</sup> which is particularly efficient for building the BWT of a highly repetitive text such as a pangenome. The algorithm also integrates Rossi et al.'s<sup>9</sup> approach for computing thresholds for repositioning.

Movi builds an index over both the forward and reverse complement of the reference sequences. This technique which was also used by SPUMONI<sup>5</sup> as it enables querying the reads in both strands simultaneously.

Movi is implemented in C++. It is GPL3-licensed open-source software available from <https://github.com/mohsenzakeri/movi>. It depends on both the prefix-free parsing implementation from the `pfp_thresholds` repository at <https://github.com/maxrossi91/pfp-thresholds> and the run splitting implementation from the `r-permute` library at <https://github.com/drnatetbrown/r-permute>. Results in this manuscript are based on the v1.0 tag of that repository.

## QUANTIFICATION AND STATISTICAL ANALYSIS

The details about the genomes used in the experiments can be found in the caption of [Tables 2](#) and [4](#). More details about the genomes and the reads are also presented in the results sections "[pseudo-matching lengths for a mock community](#)" and "[scaling to human pangenomes](#)".